Am J Transl Res 2021;13(11):12614-12625
www.ajtr.org /ISSN:1943-8141/AJTR0133182

Original Article

Injectable antimicrobial hydrogels with antimicrobial peptide and sanguinarine controlled release ability for preventing bacterial infections

Jing-Yao Liang[1,2*], Qian Li[1,2*], Long-Bao Feng[3], Sheng-Xue Hu[3], San-Quan Zhang[1,2], Chang-Xing Li[4], Xi-Bao Zhang[1,2]

[1]Institute of Dermatology, Guangzhou Medical University, Guangzhou 510095, Guangdong, China; [2]Department of Dermatology, Guangzhou Institute of Dermatology, Guangzhou 510095, Guangdong, China; [3]Beogene Biotech (Guangzhou) Co., LTD, Guangzhou 510663, Guangdong, China; [4]Department of Dermatology, Nanfang Hospital, Southern Medical University, Guangzhou 510515, Guangdong, China. [*]Equal contributors.

Received March 15, 2021; Accepted August 16, 2021; Epub November 15, 2021; Published November 30, 2021

Abstract: The emergence of antibiotic resistant bacteria represents a significant and common clinical problem worldwide as infections are becoming increasingly common. It is urgent to broaden the sources of biomaterials that can prevent both bacterial infection and antibiotic resistance. In this work, oxidized sodium alginate/aminated hyaluronic acid (OSA/AHA) hydrogel with various proportions was developed based on Schiff base reaction. Herein, polydopamine (PDA)-Bmkn2 nanoparticle and sanguinarine were incorporated into hydrogels to enhance antibacterial properties. The prepared PDA-Bmkn2 nanoparticles, with uniform particle size and good dispersion, could serve as a delivery system for Bmkn2. The prepared hydrogels showed appropriate swelling ratio, extremely good mechanical strengths and improved biodegradability. Meanwhile, the Bmkn2 and sanguinarine were released from the hydrogels in a sustainable manner. Furthermore, OSA/AHA/sanguinarine/PDA-Bmkn2 hydrogel (less than 10 μg/mL BmKn2 and 0.2 μg/mL sanguinarine) had excellent biocompatibility. Antibacterial experiments confirmed that OSA/AHA/sanguinarine/PDA-Bmkn2 hydrogel had effective antimicrobial activity on *Escherichia coli and Staphylococcus aureus.* Therefore, the prepared injectable hydrogels with good biocompatibility and excellent synergistic antibacterial activity promise great potential for preventing localized bacterial infections.

Keywords: Hydrogels, Bmkn2, sanguinarine, PDA nanoparticle, bacterial infections

Introduction

Bacterial infections are among the most prevalent and challenging conditions facing human health and the medical community [1, 2]. With advances in technology, the development of new biomaterials with the functions of preventing external pollution and tissue infection, and promoting tissue regeneration has become an intense focus of research [3]. Hydrogels, a kind of polymer with three-dimensional network structure, are widely used in regenerative medicine and biomedical applications over the past 20 years [4]. Because the hydrogels are not easy to adhere to proteins and other substances, they show good biocompatibility and nontoxicity to the human body when they are exposed to blood, body fluids and human tissues [5]. In addition, hydrogels have similar flexibility and texture of natural tissue, which can be used as human implants to reduce adverse reactions [6]. Therefore, hydrogels not only serve as a promising material for biomedical applications such as drug carriers, tissue scaffolds and biomedical devices (soft contact lenses), but also prevent further tissue damage and bacterial invasion [7]. The antibacterial hydrogels could have the double advantages of both promoting tissue regeneration and being antibacterial, which can meet the needs of biological materials [8]. Traditional antibacterial hydrogel materials loaded directly with antibiotics may lead to antibiotic resistance, which will further produce multiple drug-resistant microbes or “superbugs” [9]. Thus, it is imperative to find new antibacterial strategies.

The antibacterial mechanism of antimicrobial peptides (AMPs) is different from that of antibiotics, which is not easy to produce drug resistance [10]. AMPs, bioactive peptides encoded by host genes, are small molecular proteins that resist the invasion of pathogenic microorganisms, and remove mutated cells and carcinogens in the body [11]. Among numerous antibiotic substitutes, AMPs have attracted much attention due to their broad-spectrum antibacterial, antifungal, antiviral and immune enhancement activities [12]. The antibacterial mechanism of AMPs is to destroy the structure of bacterial cell membrane physically, which causes bacterial contents to percolate and die [13]. Bacteria are easy to mutate in a specific binding target, but it is difficult to change the composition and structure of all cell membranes. Therefore, bacteria are not easy to produce resistance to the membrane-breaking mechanism of non-specific recognition of bacterial membranes [14]. Bmkn2 has efficient antibacterial properties against Gram-negative and Gram-positive bacteria, which opens a potential new avenue for treating bacterial infections [15]. However, the AMPs are water-soluble and there is no covalent bond between the peptides and polymers, the peptides will lose quickly and become invalid [16]. Polydopamine (PDA) is a mimetic of mussel adhesive proteins containing both catechol and amine groups, which can achieve controlled drug release and drug targeting [17].

A large number of natural antibacterial components are widely known for their presence in plants and animals, such as honey, alkaloids extracted from plants, phenols and so on [18]. Alkaloids are natural compounds containing nitrogen, which can be classified as pyridine, isoquinoline, indole and so on, according to their different structures. Prior study reported that emodin extracted from rhubarb, berberine extracted from Coptis chinensis, and berberine hydrochloride have broad-spectrum antibacterial activity against Gram-negative and Gram-positive bacteria [19, 20]. Sanguinarine is a phenanthrene isoquinoline alkaloid with a molecular weight of 367.8, which has good biological effects such as antibacterial, anti-inflammatory and anti-tumor etc. [21]. Sanguinarine has broad-spectrum biological activity against *Escherichia coli*, *Pseudomonas aeruginosa* and *Staphylococcus aureus* [22]. Moreover, sanguinarine also has antibacterial activity to methicillin-resistant Staphylococcus aureus (MRSA) by affecting biofilm and bacterial lysis [23].

In this study, oxidized sodium alginate (OSA)/aminated hyaluronic acid (AHA)/Bmkn2/sanguinarine hydrogel with good biocompatible and antibacterial function was prepared based on chemical cross-linking reaction (Schiff base reaction) on a natural composite substrate. Sodium alginate (SA) is an acidic linear polysaccharide, which has excellent biodegradability, biocompatibility, porosity, and hydrophilicity [24, 25]. Hyaluronic acid (HA) is a linear hydrophilic polysaccharide, naturally occurring in the extracellular matrix (ECM) of most tissues, which can already be found in many applications in the medical field due to its excellent biocompatibility and good bioresorbability [26]. Furthermore, PDA nanoparticles were used as drug carriers of BmKn2 to improve the sustained release function. The swelling ratio, rheological properties, mechanical strengths *in vitro* drug release studies and degradation were evaluated. Moreover, the cytotoxicity of the prepared hydrogels was evaluated by using L929 fibroblasts. The antimicrobial activities of the prepared hydrogels were evaluated by using *E. coli* and *S. aureus*. We hope that the prepared hydrogels have great potential for biomedical applications.

Materials and methods

Materials

Sodium alginate (SA), sanguinarine, dopamine hydrochloride, adipic dihydrazide (ADH), hydroxy-benzotriazole (HOBt), 1-ethyl-3-(3-dimethylaminopropyl)-carbodiiminde (EDC) and N-hydroxysuccinimide (NHS) were purchased from Macklin Biochemical Co., Ltd (Shanghai, China). Hyaluronic acid (HA, MW =200 kDa) was obtained from Bloomage Biotech Co., Ltd. (Shangdong, China). BmKn2 antimicrobial peptide (purity >98%) was obtained from Apeptide Bio-Technology Co., Ltd. (Shanghai, China). Sodium periodate was purchased from Tianjin DaMao Chemical Reagent Factory (Tianjin, China). Sodium chloride was purchased from Sinopharm Chemical Reagent Co., Ltd. L929 fibroblast cell line was obtained from Dingguo Biotechnology Co., Ltd. (Beijing, China). Cell Counting Kit-8 (CCK-8) and LIVE/DEAD cell

Table 1. Preparation and orthogonal screening of OSA/AHA hydrogels

Group	G1	G2	G3	G4	G5	G6	G7	G8	G9
OSA concentration	15%	15%	15%	20%	20%	20%	25%	25%	25%
AHA concentration	2%	3%	4%	2%	3%	4%	2%	3%	4%

imaging kit was obtained from Biyuntian Biotechnology CO. LTD. (Shanghai, China). These reagents were used without further purification.

Synthesis of polymers

Synthesis of PDA nanoparticles: Dopamine (500 mg) was dissolved in 10 mL deionized water and then slowly dropped to mixed solutions (consisted of 90 mL deionized water, 40 mL ethanol and 2 ml ammonia). After reacting for 4-5 h at room temperature, the pH of above solutions was adjusted to 6.5. The precipitation was then collected by centrifugation at 14000 r/min for 10 min at 4°C. After wash three times with deionized water, the precipitation was redispersed in deionized water. Finally, the macromolecular PDA was removed by centrifugation at 4000 r/min for 5 min, and the upper solution was freeze-dried to prepare PDA nanoparticles.

Synthesis of PDA-BmKn2 nanoparticles: BmKn2 (10 mg) and EDC (10 mg) were dissolved in 5 mL PBS (pH=5.5). After stirring for 15 min at room temperature, NHS (15 mg) was added to the above solution, and then 10 mL PBS (pH=7.4) was added. The pH was adjusted to 6.8-7.2 using 0.1 mol/L hydrochloric acid solution or 0.1 mol/L NaOH solution. After stirring for 15 min, PDA (10 mg) was dissolved in water/DMSO/1 mol/L hydrochloric acid (10:4:1, v:v:v) and added dropwise into the above solution. After reacting for 4 h in an ice bath, the PDA-BmKn2 solution was dialyzed using dialysis bag (MWCO 1000) against deionized water for 4 h. The obtained PDA-BmKn2 nanoparticles were lyophilized and stored at 4°C until further use. The drug loading capacity (LC) was calculated using the following formula: Loading Capacity (%) = (The mass of loaded BmKn2)/(The total mass of *PDA-BmKn2* nanoparticles) ×100%.

Synthesis of OSA: OSA was synthesized as described previously with slight modifications [27]. First, sodium alginate (5 g) was added to 200 mL deionized water, followed by the addition of 50 mL absolute ethanol. Sodium periodate (5 g) was added to the above solution under light-shielded conditions, and after reacting for 24 h, 2 mL ethylene glycol was added to quench the oxidation reaction. NaCl (5 g) was added and the mixture was poured in 1000 mL of absolute ethyl alcohol, and the white solid was precipitated. Subsequently, the precipitation was harvested by filtering and dissolved in deionized water. Finally, the obtained solution was dialyzed using dialysis bag (MWCO 8000) against deionized water for 3 days. The OSA monomer was obtained after lyophilized for 2 days.

Synthesis of AHA: AHA was synthesized according to the reported procedure with slight modifications [28]. HA (0.5 g) and ADH (10 g) were dissolved in 100 mL deionized water. Subsequently, 10 mL DMSO/H_2O solution (1:1, v:v) with EDC (0.8 g) and HoBt (0.7 g) were added in above HA solutions and adjusted the pH to 5.0. After reacting for 24 h, NaCl (5 g) was added and the mixture was poured in 1000 mL of absolute ethyl alcohol, and the white solid was precipitated. Subsequently, the precipitation was harvested by filtering and dissolved in deionized water. Finally, the obtained solution was dialyzed using dialysis bag (MWCO 3500) against deionized water for 3 days. The AHA monomer was obtained after lyophilized for 2 days.

Preparation of hydrogels

OSA (15, 20, 25, wt%) and AHA (2, 3, 4, wt%) were fully dissolved in PBS, respectively. The OSA/HAH hydrogel was formed by mixing at the volume ratio of OSA/AHA (1:2). The groups of prepared hydrogels were shown in **Table 1**. To prepare *Sanguinarine* + *BmKn2* loaded hydrogel, PDA-BmKn2 *nanoparticle*s (the final concentration of pure BmKn2 in OSA/HAH was 0, 5, 10, 20 and 40 μg/mL) was added into AHA solution, followed by mixed OSA and Sanguinarine (the final concentration of Sanguinarine in OSA/HAH was 0, 0.1, 0.2, 0.4 and 0.8 μg/mL) solutions to prepare the OSA/HAH/Sanguinarine/PDA-BmKn2 hydrogels.

Characterization of the synthesized materials

The Fourier transform infrared spectroscopy (FTIR) spectra of PDA, PDA-BmKn2, SA, OSA, HA, AHA, and OSA/AHA were recorded with FTIR spectroscopy (VERTEX70, Bruker, Germany) in the range of 600-4000 cm^{-1}. Transmission electron microscope (TEM) images of PDA and PDA-BmKn2 nanoparticles were obtained on an electron microscope (H-800, Hitachi, Japan). The hydrodynamic sizes of PDA and PDA-BmKn2 nanoparticles were measured with the dynamic light scattering technique using Zetasizer (Nano-ZS 90, Malvern, UK).

The gelation time of hydrogel

The gelation time of hydrogel was determined by the vial-tilting method [29]. The precursor solutions of OSA and AHA were mixed gently at 37°C. The gelation time was determined when there is no liquid flowing out. All the gelling times were repeated at least three times for each group.

Swelling ratio of the hydrogels

The swelling behaviour of hydrogels was evaluated by the equilibrium swelling ratio (ESR) [30]. Test hydrogels were weighted immediately and then immersed in phosphate-buffered saline (PBS, pH=7.4). At predetermined time intervals (1, 3, 5, 7 and 24 h), test hydrogels were removed for weighing after gently blotted with a filter paper.

The swelling ratio was calculated according to the following equation:

$$\text{Swelling ratio (\%)} = \frac{M_t - M_0}{M_0} \times 100\%$$

Where M_t and M_0 are the weight of the hydrogel at time t and time 0, respectively.

Rheological measurements

The storage modulus (G') and loss modulus (G") of test hydrogels were analyzed using a TA rheometer instrument (Kinexus, Ma Erwen instruments, Britain). G' and G" of test hydrogels were tested at shear rates ranging from 0.1 to 100 rad/s.

In vitro degradation test

The *in vitro* degradation rate of the hydrogels was measured using enzymatic degradation. Test hydrogels were initially freeze-dried and weighed prior to the study. Test hydrogels were then immersed in PBS containing either 0 U/mL or 10000 U/mL lysozyme with stirring speed of 70 rpm at 37°C. At each time point (3, 7, 14 and 21 days), test hydrogels were taken out from the degradation medium, freeze-dried and weighed. The weight loss rate of hydrogels was calculated using the following equation:

$$\text{Weight loss ratio (\%)} = W_t/W_0 \times eig$$

Where W_t and W_0 are the final and initial weight of the hydrogel after degradation, respectively.

In vitro drug release studies

The standard calibration curves: The ultraviolet (UV) absorbance was detected at 205 nm and the standard calibration curves of BmKn2 were constructed using eight concentrations (50, 40, 30, 20, 10, 5, 2.5 and 1.25 μg/mL). The UV absorbance was detected at 276 nm and the standard calibration curves of sanguinarine were constructed using six concentrations (25, 20, 15, 10, 5 and 2.5 μg/mL).

In vitro drug release test of hydrogels

Test hydrogels were immersed in 10 mL PBS solution with stirring speed of 70 rpm at 37°C. At predetermined time points, 1 mL release medium of the sample was collected and 1 mL of fresh medium was added. The concentration of the BmKn2 and sanguinarine was determined by an Ultramicro ultraviolet spectrophotometer (UV-1800, Shimadzu, Japan) at λ_{max} of 205 and 276 nm, respectively. The release behavior of the drug-loaded hydrogel was continuously determined for 7 days.

In vitro biocompatibility test

The cytotoxicity of the hydrogels was evaluated through the CCK-8 assay using leaching solution method. The prepared hydrogels were soaked in DMEM supplemented with 10% FBS, 100 units/mL penicillin and 100 mg/mL streptomycin at the ratio of 0.1 g:1 mL to prepare leaching solution at 37°C for 24 h. Subsequently, 500 μL of L929 cells suspension with cell density of 2×10^4 cells/mL was seeded on a 48-well plate, and then incubated at 37°C in a humidified atmosphere incubator containing 5% CO_2. After 12 h, culture medium was replaced with 500 μL of leaching solution.

The leaching solution was removed after 24 h and washed with PBS for three times. The viability of L929 cells after culture with leaching solution was assessed by the live/dead staining and CCK-8 assay.

For the CCK-8 assay, the cell culture medium was replaced with 500 μL of fresh medium containing 10% CCK-8. After incubation at 37°C for 1-2 h, the absorbance was measured at 450 nm using a microplate reader (MultiskanMK3, Thermo, USA). For the live/dead staining, the cell culture medium was replaced with 500 μL of live/dead staining stock solution. After incubation at 4°C for 15 min, the stained cells were visualized with a fluorescent microscope (BM3000D, Shanghai Qibu Bio Tech Co., Ltd, China). The steps of cell viability assay in BmKn2 and sanguinarine were the same as those described above, except for the treatment with BmKn2 at different concentrations (0, 5, 10, 20 and 40 μg/mL) and sanguinarine at different concentrations (0, 0.1, 0.2, 0.4 and 0.8 μg/mL).

In vitro antimicrobial activity assay

The antibacterial properties of hydrogels were evaluated using Gram-positive *Staphylococcus aureus* (*S. aureus*, ATCC6538) and Gram-negative *Escherichia coli* (*E. coli*, ATCC25922). Test hydrogels and 1.8 mL bacterial suspensions with density of 1×10^6 CFU/mL were co-cultured in a 24-well plate at 37°C for 4 h. Then, 100 μL of bacterial suspensions were serially diluted and plated on LB agar plates. After incubation for 24 h at 37°C, the number of colonies was counted. The antibacterial rate (AR) of hydrogels was calculated using the following equation:

$$AR(\%) = \frac{N_c - N_s}{N_c} \times 100$$

Where N_S and N_C are the number of colonies in the hydrogel sample and the control, respectively.

Statistical analysis

All data were shown as mean ± standard deviation (SD). Significant differences were determined using one-way analysis of variance. Significant difference was defined at *P<0.05, **P<0.01, and ***P<0.001.

Results and discussion

Characterization of nanoparticles

Typical TEM imaging revealed that the resultant PDA and PDA-BmKn2 nanoparticles were irregularly shaped nanoparticles with a uniform distribution (**Figure 1A** and **1B**). Moreover, the average hydrodynamic diameter of PDA and PDA-BmKn2 obtained by dynamic light scattering (DLS) test was 292±4.9 nm with PDI of 0.261 (**Figure 1C**) and 328.7± 25.6 nm with PDI of 0.387 (**Figure 1D**), which finding was basically consistent with TEM results. As shown in Figure S1, PDA-BmKn2 nanoparticles were stable in PBS solution. We also determined hydrodynamic diameters of PDA-BmKn2 nanoparticles in PBS solution, which remained stable for 5 days. The Fourier transform infrared (FTIR) spectra of PDA and PDA-BmKn2 are shown in **Figure 2A**. There are more phenolic hydroxyl and imine in PDA nanoparticles; the broad absorption peak at 3400-3600 cm^{-1} is the result of the superposition of phenolic hydroxyl and imine. The absorption peak at 1516 cm^{-1} is assigned to be the bending vibration absorption peak of imine. The bending vibration absorption of imine structure on common hydrocarbons is very weak, but the imine group in the dopamine molecule is strongly absorbed due to the formation of large π bond between imino group and benzene ring. PDA-BmKn2 nanoparticles show double peaks at around 3530 cm^{-1} and 3462 cm^{-1}, which belong to the absorption peak of amino group in BmKn2. A strong absorption peak at 1637 cm^{-1} is assigned to the absorption peak of carbonyl group on amide bond. Meanwhile, BmKn2 molecule is a polypeptide composed of 13 amino acids with more amide structure, and there is no absorption peak at 1516 cm^{-1} in PDA-BmKn2, which indicates that BmKn2 is successfully connected to PDA molecule.

Characterization of hydrogels

The FTIR spectra of SA, OSA, HA, AHA and OSA/AHA are shown in **Figure 2B**. There are many interactional hydroxyl groups in sodium alginate (SA), which show a wide peak at 3410 cm^{-1}. However, the absorption peak of hydroxyl group in OSA is significantly weaker than that of SA. Meanwhile, the association between the

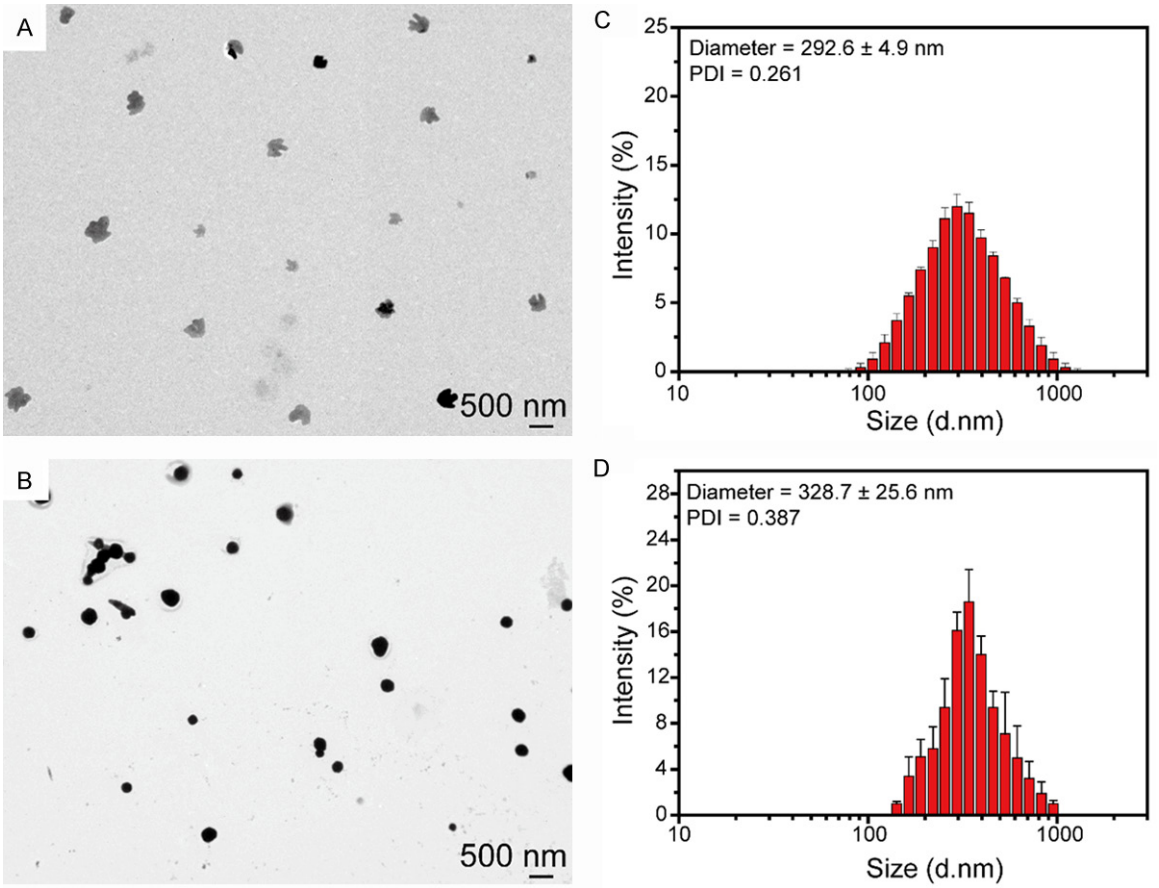

Figure 1. A. TEM images of PDA; B. TEM images of PDA-BmKn2; C. Size distribution of PDA; D. Size distribution of PDA-BmKn2.

hydroxyl groups in OSA is weakened, and the absorption peak moves to the high wave number, which proves that some hydroxyl groups in sodium alginate are oxidized to aldehyde group [31]. A large number of amino groups were added to the HA structure after the reaction of HA with ADH, a broad peak in AHA appeared at 3512 cm^{-1} is corresponded to an amino absorption peak, which proves the successful reaction of HA with ADH. The Schiff base reaction in OSA/AHA hydrogel will consume aldehyde group and amino group. The absorption peak in OSA/AHA at 1714 cm^{-1} disappeared and the absorption peak at 3512 cm^{-1} shifted, which proved the successful reaction of OSA with AHA. **Figure 2C1** and **2C2** showed that the process of the sol-gel process of the OSA/AHA hydrogel in PBS was transparent and yellowish in color. **Figure 2C3** showed the macroscopic images of OSA/AHA, OSA/AHA/BmKn2, OSA/AHA/sanguinarine and OSA/AHA/BmKn2/sanguinarine hydrogels. **Figure 2D** showed the gelation time test results of the OSA/AHA hydrogels with different proportions of mass of OSA and AHA. It can be seen from the figure that the gelation time of G2 and G7 hydrogels is about 60 s, which might be suitable as the application of injectable hydrogels.

Swelling ratio of hydrogels

As shown in **Figure 3A**, the hydrogel with different concentration ratio absorbs and expands in the first 6 h. After 7 h of incubation, equilibrium swelling was achieved in G1-G9 hydrogels. The weight remains basically unchanged after 7 h, and the swelling ratio of G1-G9 is between 70% and 200%, which can be used as hydrogel drug loading system. Considering the gelation time and strength of hydrogel, 25% OSA/2% AHA hydrogel was selected as the drug loading system, and the swelling rate of hydrogel was about 200%. This high swelling rate was due to the factor that OSA and AHA have many hydrophilic groups which can absorb

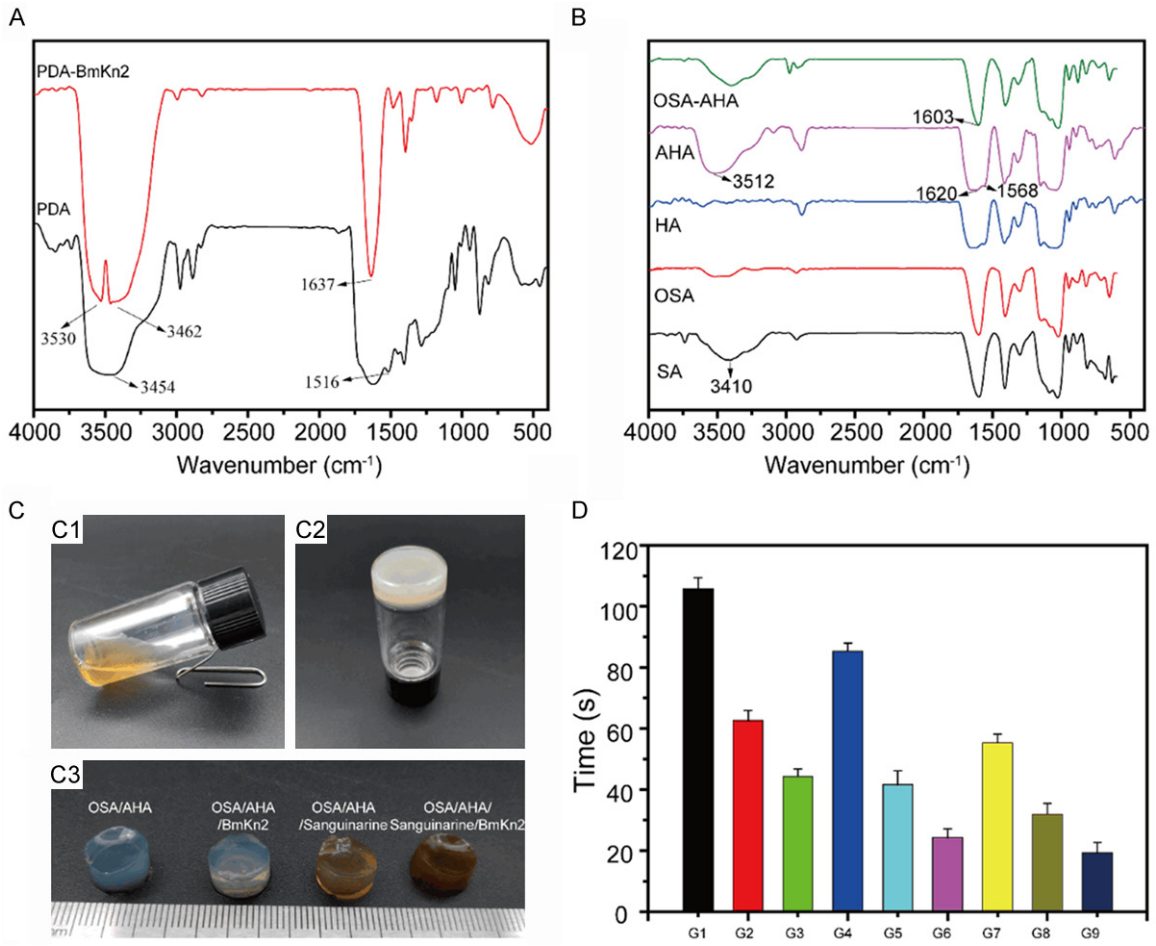

Figure 2. A. FTIR spectra of PDA and PDA-BmKn2; B. FTIR spectra of SA, OSA, HA, AHA and OSA/AHA; C. Photograph of the OSA/AHA hydrogel; D. Gelation time of the OSA/AHA hydrogels with different proportions.

large amounts of water molecules, and free water can enter into easily a three-dimensional network structure in the hydrogel [28]. The drug loaded hydrogels is shown in **Figure 3B**. compared to the pure hydrogel, the swelling rate of PDA-BmKn2 loaded hydrogel (174%) decreases slightly and the swelling rate of sanguinarine loaded hydrogel (189%) is basically unchanged. However, the swelling rate of the PDA-BmKn2 and sanguinarine loaded hydrogel (132%) decreases obviously. The decreased swelling rate could be due to the hydrogel network becoming more compact with the drug added. Our results showed that prepared hydrogels possessed adjustable swelling rate, which was adapted to various environments *in vivo*.

Rheological analysis

The rheological property of G1-G9 hydrogels is shown in **Figure 3C**. When the elastic modulus (G') is greater than the viscous modulus (G"), it shows ransition from the solution state to hydrogel state. The G' of each group is basically greater than the G" from the beginning. The extent of gelation increases with time, the G' increases greatly, and the change of G" is relatively small. All results indicated that the G1-G9 hydrogels are stable and exhibit good mechanical properties.

Examination of degradation rate

The biodegradation of the 25% OSA/2% AHA hydrogel was studied by lysozyme hydrolysis. As shown in **Figure 3D**, the degradation rate of hydrogel with lysozyme was significantly faster than that without lysozyme. The degradation rate of hydrogel was faster in the first 3 days, and the degradation rate of hydrogel with and without lysozyme was 67% and 54%, respectively. At 21 days, the degradation rate of hydro-

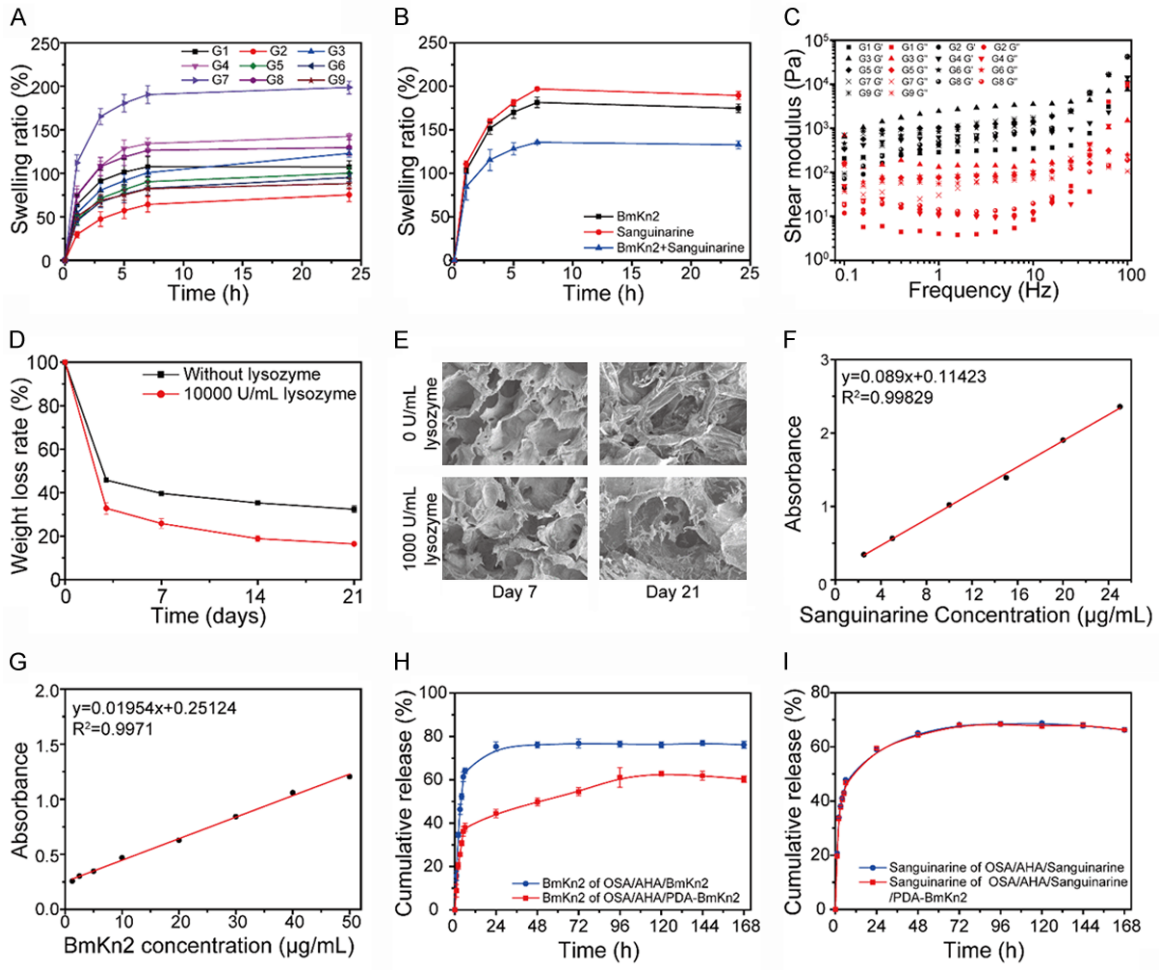

Figure 3. A. Swelling ratio of the OSA/AHA hydrogels with different proportions; B. Swelling ratio of the different drug loaded hydrogels; C. The rheological properties of the OSA/AHA hydrogels with different proportions; D. The weight loss ratio of 25% OSA/2% AHA hydrogels in PBS solution, either in the presence or absence of 10000 U/mL lysozyme; E. SEM images of the surface morphology of 25% OSA/2% AHA hydrogels during degradation; F. Standard curve of sanguinarine; G. Standard curve of Bmkn2; H. The cumulative release curve of Bmkn2; I. The cumulative release curve of sanguinarine.

gel without lysozyme was 68%. However, the degradation rate of hydrogel with lysozyme was 84% at 21 days, which was basically degraded completely. The morphologies of degraded 25% OSA/2% AHA hydrogel was also observed by SEM (**Figure 3E**), and the fragments in hydrogels increased with incubation time. These results confirmed that 25% OSA/2% AHA hydrogel have good stability under enzymatic hydrolysis, thus prolong duration of use and reduing the frequency of routine materials replacement.

In vitro drug release studies

The standard curve of sanguinarine and BmKn2 is shown in **Figure 3F** and **3G**. The drug loading of BmKn2 in PDA-BmKn2 nanoparticles was about 13.5±1.3%. The drug release curve of the hydrogels is shown in **Figure 3H** and **3I**. 59% of sanguinarine and 47% of BmKn2 were released within 1 day. All hydrogels have a relatively fast release at the early stage, which was mainly due to an amount of BmKn2 and sanguinarine on the surface of hydrogels. Afterward, the drug release rate declined, nearly 30% of sanguinine and 35% of BmKn2 were un-released in hydrogels even after 7 days. The release process of BmKn2 in BmKn2 loaded hydrogels was slower than that of sanguinarine, which was caused by double drug delivery system between PDA nanoparticle and hydrogel matrix.

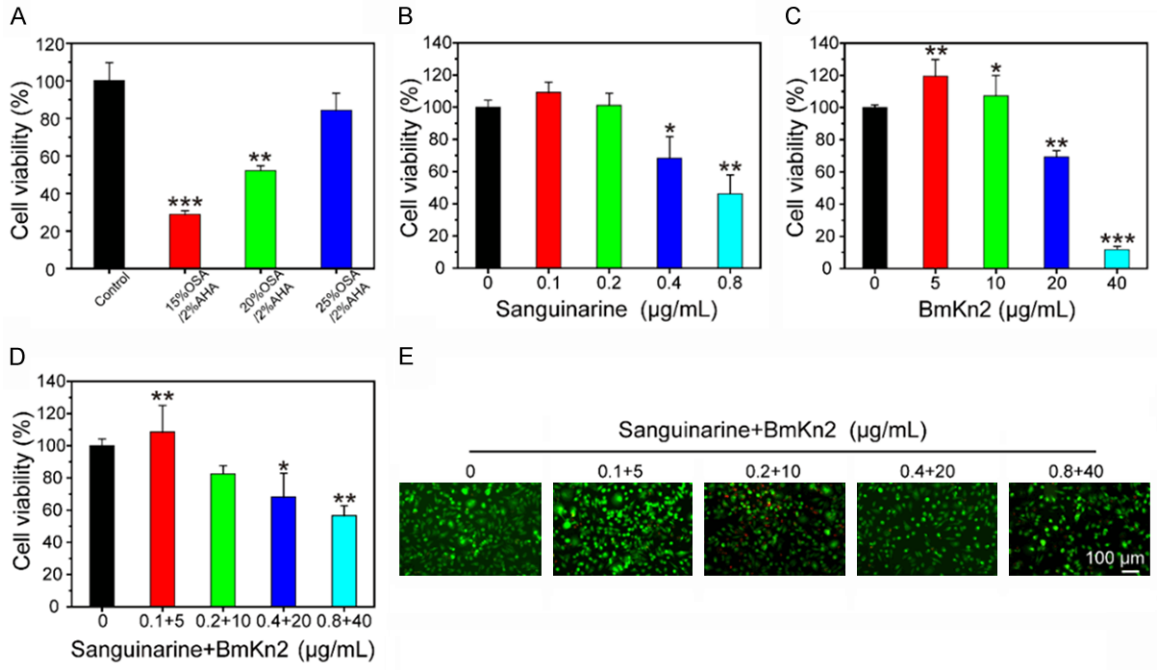

Figure 4. A. Viability of L929 cells of the OSA/AHA hydrogels with different proportions assessed using CCK-8 assays; B. Cell viability with sanguinarine at different concentrations; C. Cell viability with Bmkn2 at different concentrations; D. Cell viability with the OSA/AHA/sanguinarine/PDA-Bmkn2 hydrogels; E. Fluorescence images of L929 cells after live/dead staining.

In vitro biocompatibility test

To determine whether hydrogels are suitable for application *in vivo*, it is important to consider not only its physical properties but also its cytotoxicity. The biocompatibility test of the hydrogel material is shown in **Figure 4A**. The cell viability of 15% OSA/2% AHA, 20% OSA/2% AHA and 25% OSA/2% AHA hydrogel is 28±2%, 52±3% and 84±9%, respectively. The cytotoxic of 25% OSA/2% AHA hydrogel can be ignored, which is selected as optimal materials. It was mainly due to the use of SA and HA with excellent biocompatibility, without the use of traditional biotoxicity crosslinkers. As shown in **Figure 4B-D**, when the concentration of BmKn2 is less than 10 μg/mL and the concentration of sanguinarine is less than 0.2 μg/mL, the hydrogel system loaded with BmKn2, sanguinarine and double-loaded BmKn2 and sanguinine can meet the requirements. BmKn2 and sanguinarine (as antimicrobial agent) can damage normal cells to a certain extent, but at safe concentrations it will not cause serious adverse effect on normal cells [32, 33]. The cell viability of hydrogels was further assessed using l/Ddead staining. As shown in **Figure 4E**, the alive cells cultured in the leaching solution of hydrogels (less than 10 μg/mL BmKn2 and 0.2 μg/mL sanguinarine) were comparable to the control group with the cells seeded in the cell culture medium. The OSA/AHA hydrogel in this study is prepared by Schiff base reaction, which avoids the possible cytotoxicity caused by the introduction of free radical cross-linking agent in traditional methods [24].

In vitro antibacterial property

High-quality biomaterials not only have great biocompatibility to promote tissue regeneration, but also have excellent antibacterial properties to prevent tissue infection. Here, *E. coli* and S. *aureus* were chosen to evaluate the antimicrobial properties of these hydrogels using surface antibacterial activity tests. As shown in **Figure 5A** and **5B**, OSA/AHA/sanguinarine/PDA-Bmkn2 hydrogel with 10 μg/mL BmKn2 and 0.2 μg/mL sanguinarine possess the best antibacterial properties, which could kill about 100% of *E. coli* and 100% of S. *aureus* attributed to the synergistic antibacterial effect of BmKn2 and sanguinarine. Meanwhile, OSA/

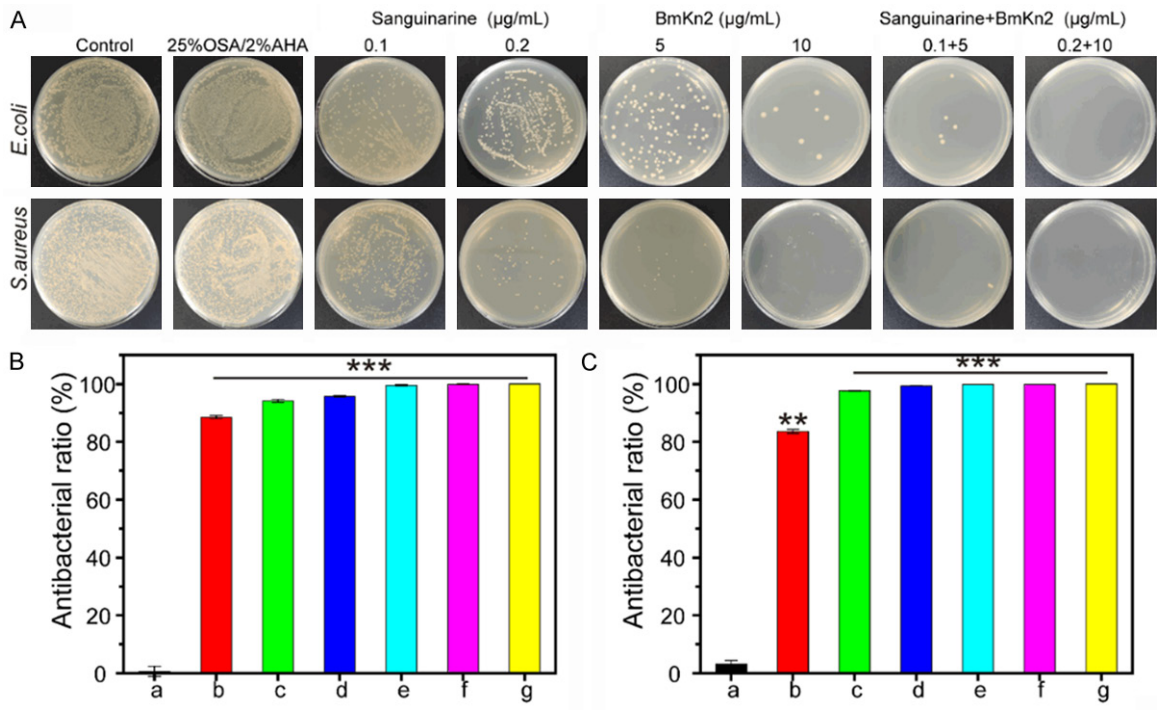

Figure 5. (A) Bacterial colonies of *E. coli* and *S. aureus* after coculture with 25% OSA/2% AHA, OSA/AHA/sanguinarine (0.1 μg/mL), OSA/AHA/sanguinarine (0.2 μg/mL), OSA/AHA/Bmkn2 (5 μg/mL), OSA/AHA/Bmkn2 (10 μg/mL), OSA/AHA/sanguinarine (0.1 μg/mL)/Bmkn2 (5 μg/mL) and OSA/AHA/sanguinarine (0.1 μg/mL)/Bmkn2 (10 μg/mL) hydrogels, respectively. (B, C) Antibacterial ratio of *E. coli* (B) and *S. aureus* (C), respectively.

AHA/sanguinarine/PDA-Bmkn2 hydrogel with 5 μg/mL BmKn2 and 0.1 μg/mL sanguinarine could kill about 99.9% of *E. coli* and 99.9% of *S. aureus*. Considering the toxicity of Hydrogels at the highest concentration tested (10 μg/mL BmKn2 and 0.2 μg/mL sanguinarine), OSA/AHA/sanguinarine/PDA-Bmkn2 hydrogel with 5 μg/mL BmKn2 and 0.1 μg/mL sanguinarine was selected as the most suitable materials. Prior study reported that sanguinarine may induce the release of autolysin from the cell wall of bacteria, leading to cell lysis and diaphragm. The minimum inhibitory concentration (MIC) ranges from 3.12 μg/mL to 6.25 μg/mL [34].

Conclusions

In summary, we herein designed an injectable hydrogel with antimicrobial peptide and sanguinarine controlled release ability to combat drug-resistant bacterial infections in the healthcare settings. OSA/AHA/sanguinarine/PDA-Bmkn2 hydrogel was prepared successfully by a Schiff-base reaction under mild conditions. The hydrogel showed suitable gelation time, appropriate swelling ratio, stable rheological properties, extremely good mechanical strengths and the stability of enzymatic degradation. The *in vitro* release data showed that hydrogel had a good ability for drug retention and the Bmkn2 was released from PDA nanoparticle and hydrogel matrix in a sustained and slow manner. OSA/AHA/sanguinarine/PDA-Bmkn2 hydrogel (less than 10 μg/mL BmKn2 and 0.2 μg/mL sanguinarine) exhibited good biocompatibility. Meanwhile, OSA/AHA/sanguinarine/PDA-Bmkn2 hydrogel with 5 μg/mL BmKn2 and 0.1 μg/mL sanguinarine had potent antibacterial properties. Taking into consideration of the results, the prepared OSA/AHA/sanguinarine/PDA-Bmkn2 hydrogel with 5 μg/mL BmKn2 and 0.1 μg/mL sanguinarine may be considered as a new antibacterial candidate for the surgical site infection application. Moreover, by using PDA nanoparticle and hydrogel systems, various drugs can be loaded in hydrogel matrices to prepare multifunctional materials with sustaining drug release properties.

Acknowledgements

This study was supported by the Natural Science Foundation of Guangdong (Grant No. 2018A0303130011 and 2013B021800035),

the Science and Technology Program of Guangzhou (Grant No. 201904010191), the Characteristic Clinic Project of Guangzhou Health Commission (Grant No. 2019TS68), the Medical Science and Technology Research Foundation of Guangdong Province (Grant No. A2019464).

Disclosure of conflict of interest

None.

Address correspondence to: Dr. Xi-Bao Zhang, Institute of Dermatology, Guangzhou Medical University, Guangzhou 510095, Guangdong, China. Tel: +86-20-83593476; E-mail: gzpfbfzs@163.com; Dr. Chang-Xing Li, Department of Dermatology, Nanfang Hospital, Southern Medical University, Guangzhou 510515, Guangdong, China. Tel: +86-20-61641989; E-mail: 58632342@qq.com

References

[1] Roewe J, Stavrides G, Strueve M, Sharma A, Marini F, Mann A, Smith S, Kaya Z, Strobl B, Mueller M, Reinhardt C, Morrissey J and Bosmann M. Bacterial polyphosphates interfere with the innate host defense to infection. Nat Commun 2020; 11: 4035.

[2] Yang C, Luo Y, Lin H, Ge M, Shi J and Zhang X. Niobium carbide MXene augmented medical implant elicits bacterial infection elimination and tissue regeneration. ACS Nano 2021; 15: 1086-1099.

[3] Pang Q, Lou D, Li S, Wang G, Qiao B, Dong S, Ma L, Gao C and Wu Z. Smart flexible electronics-integrated wound dressing for real-time monitoring and on-demand treatment of infected wounds. Adv Sci (Weinh) 2020; 7: 1902673.

[4] Loebel C, Rodell CB, Chen MH and Burdick JA. Shear-thinning and self-healing hydrogels as injectable therapeutics and for 3D-printing. Nat Protoc 2017; 12: 1521-1541.

[5] Meng C, Wei W, Wang Y, Zhang K, Zhang T, Tang Y and Tang F. Study of the interaction between self-assembling peptide and mangiferin and in vitro release of mangiferin from in situ hydrogel. Int J Nanomedicine 2019; 14: 7447-7460.

[6] Chatterjee S and Chi-Leung Hui P. Review of stimuli-responsive polymers in drug delivery and textile application. Molecules 2019; 24: 2547.

[7] Townsend J, Beck E, Gehrke S, Berkland C and Detamore M. Flow behavior prior to crosslinking: the need for precursor rheology for placement of hydrogels in medical applications and for 3D bioprinting. Prog Polym Sci 2019; 91: 126-140.

[8] Nimal T, Baranwal G, Bavya M, Biswas R and Jayakumar R. Anti-staphylococcal activity of injectable nano tigecycline/chitosan-PRP composite hydrogel using drosophila melanogaster model for infectious wounds. ACS Appl Mater Interfaces 2016; 8: 22074-22083.

[9] Wang J, Feng L, Yu Q, Chen Y and Liu Y. Polysaccharide-based supramolecular hydrogel for efficiently treating bacterial infection and enhancing wound healing. Biomacromolecules 2021; 22: 534-539.

[10] Zhu Y, Shao C, Li G, Lai Z, Tan P, Jian Q, Cheng B and Shan A. Rational avoidance of protease cleavage sites and symmetrical end-tagging significantly enhances the stability and therapeutic potential of antimicrobial peptides. J Med Chem 2020; 63: 9421-9435.

[11] Lee E, Zhang C, Di Domizio J, Jin F, Connell W, Hung M, Malkoff N, Veksler V, Gilliet M, Ren P and Wong G. Helical antimicrobial peptides assemble into protofibril scaffolds that present ordered dsDNA to TLR9. Nat Commun 2019; 10: 1012.

[12] Cao J, Zhang Y, Shan Y, Wang J, Liu F, Liu H, Xing G, Lei J and Zhou J. A pH-dependent antibacterial peptide release nano-system blocks tumor growth in vivo without toxicity. Sci Rep 2017; 7: 11242.

[13] Plisson F, Ramírez-Sánchez O and Martínez-Hernández C. Machine learning-guided discovery and design of non-hemolytic peptides. Sci Rep 2020; 10: 16581.

[14] Bao Y, Wang S, Li H, Wang Y, Chen H and Yuan M. Characterization, stability and biological activity in vitro of cathelicidin-BF-30 loaded 4-Arm star-shaped PEG-PLGA microspheres. Molecules 2018; 23: 497.

[15] Cao L, Dai C, Li Z, Fan Z, Song Y, Wu Y, Cao Z and Li W. Antibacterial activity and mechanism of a scorpion venom peptide derivative in vitro and in vivo. PLoS One 2012; 7: e40135.

[16] He Y, Jin Y, Wang X, Yao S, Li Y, Wu Q, Ma G, Cui F and Liu H. An antimicrobial peptide-loaded gelatin/chitosan nanofibrous membrane fabricated by sequential layer-by-layer electrospinning and electrospraying techniques. Nanomaterials (Basel) 2018; 8: 327.

[17] Chen C, Martin-Martinez F, Jung G and Buehler M. Polydopamine and eumelanin molecular structures investigated with ab initio calculations. Chem Sci 2017; 8: 1631-1641.

[18] Hossain M, Polash S, Takikawa M, Shubhra R, Saha T, Islam Z, Hossain S, Hasan M, Takeoka S and Sarker S. Investigation of the antibacterial activity and in vivo cytotoxicity of biogenic silver nanoparticles as potent therapeutics. Front Bioeng Biotechnol 2019; 7: 239.

[19] Su P, Yang C, Yang J, Su P and Chuang L. Antibacterial activities and antibacterial mechanism of polygonum cuspidatum extracts against nosocomial drug-resistant pathogens. Molecules 2015; 20: 11119-11130.
[20] Fan D, Liu L, Wu Z and Cao M. Combating neurodegenerative diseases with the plant alkaloid berberine: molecular mechanisms and therapeutic potential. Curr Neuropharmacol 2019; 17: 563-579.
[21] Zhang Q, Lyu Y, Huang J, Zhang X, Yu N, Wen Z and Chen S. Antibacterial activity and mechanism of sanguinarine against providencia rettgeri in vitro. PeerJ 2020; 8: e9543.
[22] Kudera T, Doskocil I, Salmonova H, Petrtyl M, Skrivanova E and Kokoska L. In vitro selective growth-inhibitory activities of phytochemicals, synthetic phytochemical analogs, and antibiotics against diarrheagenic/probiotic bacteria and cancer/normal intestinal cells. Pharmaceuticals (Basel) 2020; 13: 233.
[23] Zhu Q, Jiang M, Liu Q, Yan S, Feng L, Lan Y, Shan G, Xue W and Guo R. Enhanced healing activity of burn wound infection by a dextran-HA hydrogel enriched with sanguinarine. Biomater Sci 2018; 6: 2472-2486.
[24] Li H, Cheng F, Wei X, Yi X, Tang S, Wang Z, Zhang Y, He J and Huang Y. Injectable, self-healing, antibacterial, and hemostatic N,O-carboxymethyl chitosan/oxidized chondroitin sulfate composite hydrogel for wound dressing. Mater Sci Eng C Mater Bio Appl 2021; 118: 111324.
[25] Zhu Y, Kong L, Farhadi F, Xia W, Chang J, He Y and Li H. An injectable continuous stratified structurally and functionally biomimetic construct for enhancing osteochondral regeneration. Biomaterials 2019; 192: 149-158.
[26] Xu K, Yao H, Fan D, Zhou L and Wei S. Hyaluronic acid thiol modified injectable hydrogel: synthesis, characterization, drug release, cellular drug uptake and anticancer activity. Carbohydr Polym 2021; 254: 117286.
[27] Feng X, Zhang X, Li S, Zheng Y, Shi X, Li F, Guo S and Yang J. Preparation of aminated fish scale collagen and oxidized sodium alginate hybrid hydrogel for enhanced full-thickness wound healing. Int J Biol Macromol 2020; 164: 626-637.
[28] Luo P, Liu L, Xu W, Fan L and Nie M. Preparation and characterization of aminated hyaluronic acid/oxidized hydroxyethyl cellulose hydrogel. Carbohydr Polym 2018; 199: 170-177.
[29] Ke X, Li M, Wang X, Liang J, Wang X, Wu S, Long M and Hu C. An injectable chitosan/dextran/β-glycerophosphate hydrogel as cell delivery carrier for therapy of myocardial infarction. Carbohydr Polym 2020; 229: 115516.
[30] Wang X, Xu P, Yao Z, Fang Q, Feng L, Guo R and Cheng B. Preparation of antimicrobial hyaluronic acid/quaternized chitosan hydrogels for the promotion of seawater-immersion wound healing. Front Bioeng Biotechnol 2019; 7: 360.
[31] Leonaviciute G, Bonengel S, Mahmood A, Ahmad Idrees M and Bernkop-Schnürch A. S-protected thiolated hydroxyethyl cellulose (HEC): novel mucoadhesive excipient with improved stability. Carbohydr Polym 2016; 144: 514-521.
[32] Satitmanwiwat S, Changsangfa C, Khanuengthong A, Promthep K, Roytrakul S, Arpornsuwan T, Saikhun K and Sritanaudomchai H. The scorpion venom peptide BmKn2 induces apoptosis in cancerous but not in normal human oral cells. Biomed Pharmacother 2016; 84: 1042-1050.
[33] Khan A, Mohamed E, Hakeem I, Nazeer A, Kuttikrishnan S, Prabhu K, Siveen K, Nawaz Z, Ahmad A, Zayed H and Uddin S. Sanguinarine induces apoptosis in papillary thyroid cancer cells via generation of reactive oxygen species. Molecules 2020; 25: 1229.
[34] Obiang-Obounou BW, Kang OH, Choi JG, Keum JH, Kim SB, Mun SH, Shin DW, Kim KW, Park CB, Kim YG, Han SH and Kwon DY. The mechanism of action of sanguinarine against methicillin-resistant staphylococcus aureus. J Toxicol Sci 2011; 36: 277-283.

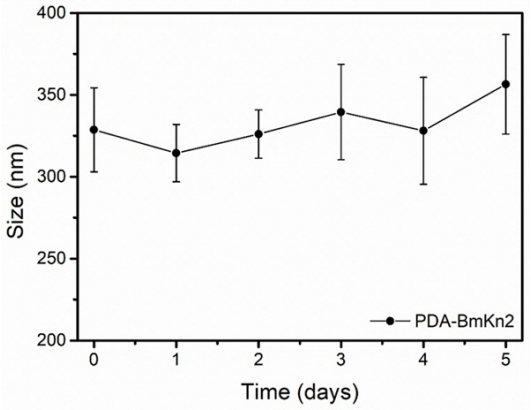

Figure S1. The size distribution of PDA-BmKn2 nanoparticles.